ROYAL SOCIETY OF CHEMISTRY

PERSPECTIVE

Check for updates

Battery electrode slurry rheology and its impact on manufacturing

Carl D. Reynolds, [iD] *[ac] Helen Walker, [iD] [b] Ameir Mahgoub,[b] Ebenezer Adebayo [iD] [b] and Emma Kendrick [iD] [ac]

The manufacturing of battery electrodes is a critical research area driven by the increasing demand for electrification in transportation. This process involves complex stages during which advanced metrology can be used to enhance performance and minimize waste. A key metrological aspect is the rheology of the electrode slurry which can give a wealth of information about the underlying microstructure and the composite slurry materials' chemical and physical properties. Despite the importance, extensive characterization and a comprehensive understanding of the relationships between rheology, microstructure, and material properties are still lacking. This work bridges academic and industrial perspectives, evaluating current advancements in characterisation. It emphasizes the role of formulation and mixing in determining the slurry's behaviour and structural properties. The study concludes with recommendations to improve measurement techniques and interpret slurry properties, aiming to optimize the manufacturing process and enhance the performance of battery electrodes.

Introduction

In the manufacture of battery electrodes, materials are mixed into a slurry, coated onto a foil current collector, dried and calendared (compressed). The aim is to produce a uniform coating, free of defects and with a consistent microstructure that promotes mechanical stability and good conductivity.[1–3]

This is a complex, multistage manufacturing process (Fig. 1), with many interdependent process parameters. It is therefore highly useful to employ metrology to get insights into the process at each stage to detect abnormalities early on before they cause knock on effects downstream. Slurry rheology, or flow properties, provides an early indicator (being applicable after slurry mixing), which can give an insight into the interactions between components, the efficiency of the mixing process and be used to predict performance in the subsequent coating. However, the slurry rheology is complex, originating from a combination of competing component interactions, and so interpretation of this behaviour can be difficult. Slurries are also a challenging material for rheological characterisation, so care needs to be taken that results are consistent and comparable.[4]

This work presents a perspective on the current progress in electrode slurry rheology, with industrial insights. First the

literature on measurement of electrode slurry rheology is reviewed, assessing the important parameters to be considered. Then the stages of manufacturing are considered, including how they determine the rheology and microstructure of the slurry and how this goes on to affect subsequent steps. Finally, recommendations are made for measurement and interpretation of slurry rheology.

Measurement of electrode slurry rheology

Rheology is most commonly studied using shear rheometers which measure the resistance to applied motion in a shear flow. The simplest test that can be performed is a flow curve (Fig. 4A), where shear is applied at different shear rates ($\dot{\gamma}$), allowed to reach steady state, and the response measured. Measurements can be made using different geometries, including cup and bob, parallel plate, and cone-cone measuring systems (Fig. 2). The measuring system is tailored to the viscosity of the material, with higher surface area geometries (*e.g.* cup/bob, large cones/plates) giving a higher force for low viscosity materials, ensuring the force is within the measurement range of the instrument.

For particle containing samples, the measurement gap is vital, and must be significantly larger than the particle size (typically an order of magnitude larger is used as a rule of thumb) to ensure there is no particle friction which gives erroneous results. Cones have a very small gap at the centre (ideally 0 but the cone tip is

a School of Metallurgy and Materials, University of Birmingham, Elms Rd, Birmingham B15 2SE, UK. E-mail: c.d.reynolds@bham.ac.uk

b UK Battery Industrialisation Centre, Rowley Rd, Baginton, Coventry CV8 3AL, UK

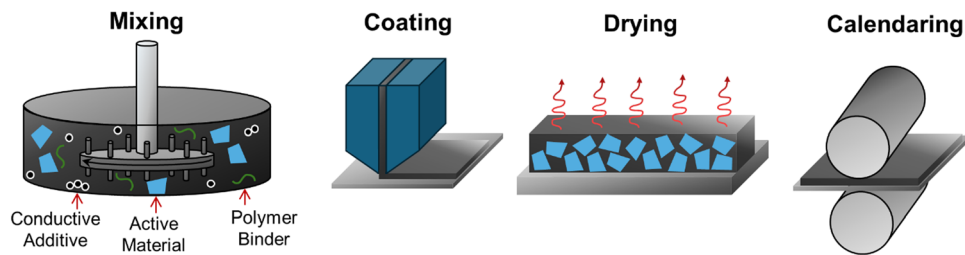*c Faraday Institution, Campus, Quad One Becquerel Avenue Harwell, Didcot OX11 0RA, UK*

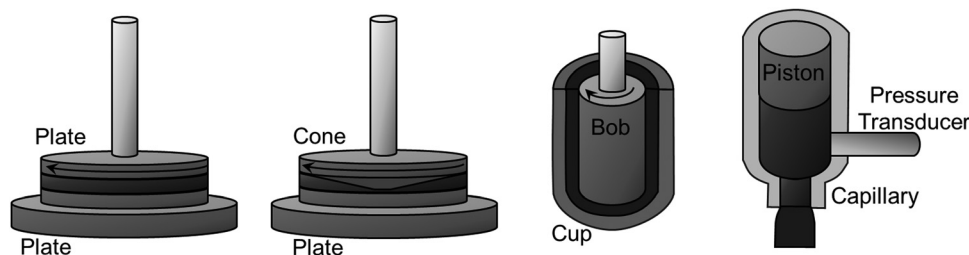**Fig. 1** Illustration of the battery electrode manufacturing process.

Fig. 2 Illustration of rheology measurement geometries, from left to right, parallel plate, cone and plate, cup and bob, capillary rheometry.

slightly truncated to prevent friction), which makes measurement of particle laden electrode slurries difficult.

However, cones also bring advantages, the shear rate is consistent across the geometry, where for a plate-plate system the shear rate is zero in the centre and highest at the edge and a correction must be applied to calculate the average shear rate. For cones, the normal force generated during shear can be used to extract the first normal stress difference. In a plate setup, the normal force contains contributions from the first and second normal stress difference which cannot be separated without additional measurement.[5] Generation of normal stresses during shear flow is a signature of elastic behaviour and the first normal stress difference is often used to quantify the viscoelasticity for modelling of the coating process, *e.g.* mild viscoelasticity has been shown to stabilise the coating bead and expand the coating window in slot die coating[6] and allow thinner coatings to be made.[7] However, at high speeds, viscoelasticity can destabilise the coating flow and cause defects.[8,9]

High shear rates are rarely measured, and most studies limit shear rates to 100 or 1000 s^{-1}, because higher shear rates bring inertial effects and sample escape from the measurement gap. The coating shear rates in the slot die head and between the head and moving current collector can be estimated and these shear rates can reach over 10 000 s^{-1}.[10,11] To achieve higher shear rates, smaller gaps can be used in a plate-plate rheometer, as the shear rate in these geometries are determined by the gap and the speed, and shear rate increases with decreasing gap for a given speed. However, care must be taken to stay well above the particle size to reduce particle friction which causes noise in the data. This can be checked by measuring at different gaps and ensuring the results overlay.

Capillary rheometers can also be used, which force the slurry through a narrow capillary and measure pressure. Again, care must be taken that the particle size is smaller than the channel to prevent blocking, but typically much higher shear rates can be achieved in this setup because it is mostly enclosed (although usually extrudes into open air), which prevents escape of the sample at high speeds.

The ideal situation would be inline monitoring. Viscosities can be extracted from in-line pressure measurements during coating, although the complex geometries used in industrial slot die coaters complicate the calculation. However, with pressure monitoring at multiple points, and correlation with offline measurements, rheology could be monitored continuously during the coating process.

Beyond viscosity, there are various other useful rheological parameters to quantify. Relaxation time is important to detect the presence of elastic instability. Relaxation time (λ) can be used to calculate a Weissenberg number (We) for the coating process where We = $\lambda\dot{\gamma}$. This can be used to quantify the 'mild' viscoelasticity that expands the coating window, where We ~ 0.1 but higher values lead to reduced coating window.[6]

Relaxation time is typically measured from oscillatory measurements, where the in phase and out of phase response to the applied strain can be measured, representing the viscous (viscous modulus G'') and elastic response (elastic modulus, G') respectively. Relaxation time can be extracted from a frequency sweep in the linear viscoelastic regime (Fig. 4B), examining the transition from flowing behaviour to elastic behaviour at increasing oscillation frequency. For electrode slurries, it can be difficult to measure at the high frequencies where this occurs due to escape of material from the parallel plate gap and inertial effects. This is typically overcome through time-temperature superposition, expanding the frequency range by performing measurements at different temperature, but this is limited for slurries as the solvent is removed quickly at higher temperatures and there is little room

for lowering the temperature before the freezing point is reached. So alternative techniques are required, for example, examining the pressure at high shear rates *e.g.* in a capillary rheometer or in-line setup, may show signatures of instability *i.e.* oscillating and not reaching a steady state, so this can be used to find the shear rate where this occurs. Relaxation after cessation of shear can also be examined (Fig. 4E), if this is performed after a deformation at high rate, then the relaxation of the stress in the material can be fitted and timescales for the different relaxations in the material can be extracted. One common test used to quantify recover after shear is a 3 interval thixotropy test, or 3ITT (Fig. 4D). This involves applying a low shear rate deformation, followed by a faster deformation and then returning to the slow rate. The recovery time of the sample viscosity can be compared easily using this technique, but it is complicated to obtain a relaxation time from these measurements because a deformation is applied throughout.

Yield stress is another key parameter, this can be measured by fitting the flow curve data, however it can also be measured directly in an amplitude sweep (Fig. 4C), where the frequency of an oscillation is fixed and the strain amplitude increased. The slurry changes from elastic behaviour to flowing behaviour and the yield stress can be extracted *via* varying procedures. The first change from a plateau in G' and G'' can be measured, which represents the start of of network breakdown and structural change. The crossover in G' and G'' can be used, as the point at which the slurry will start to flow. Finally, the peak in the elastic component of the stress σ' can be used, which has been shown to be most reproducible and comparable to other methods of yield stress determination.[12,13] Care must be taken when using the yield stress values that the method of determining them is consistent, as the values extracted vary significantly between these methods and represent different stages of yielding.

Shear is only one of the two components of flow, the other being extension. Shear generates a velocity gradient perpendicular to the motion applied, whereas extension generates a parallel velocity gradient (Fig. 3). The majority of complex flows, *e.g.* in a slot die head, have both shear and extensional components. Therefore, it is important to consider behaviour in both modes.

Often the drivers of shear rheology and extension are the same, and the two properties correlate, however this is not always the case. Branched polymer binders, while having high shear viscosity, show even higher extensional viscosity as branch points promote chain stretching in extension.[14] Yield stress in extension is also shown to be significantly higher than in shear.[15] Extensional rheology unfortunately is limited in commercial apparatus available for measurement. It can be measured using capillary breakup rheometry, filament stretching rheometry (both of which typically use custom setups), or the use of exit and entry dies in a commercial capillary rheometer to estimate the extensional viscosity, although there approximations are needed for this, and it does not always match the viscosity in pure extensional flows.[16,17]

Surface properties

While discussing slurry rheology, it is also useful to highlight surface properties. The surface tension and surface energy between slurry and current collector are also highly important to the flow in the coater. However, surface properties of slurries are rarely measured, partly because of difficulty in their reproducible determination. They are particularly important for lower weight solids slurries, where the forces generated by surface energy can equal or outweigh the rheological response during coating. For highly viscous and elastic slurries, the effect of surface tension becomes smaller, but it is still necessary to quantify for physical modelling.

There are various methods for determining surface tension, including pull force methods, where a geometry such as a Wilhelmy plate or de Nuoy ring (Fig. 5) is immersed into the liquid surface and pulled out, and the force on the geometry measured. Wilhelmy plate performs better for viscous materials like electrode slurries and does not require knowledge of the liquid density and correction (in ring methods a correction factor for the difference in shape between the inner and outer ring surface must be used. However care must be taken that the plate is minimally submerged, or else corrections for buoyancy must be applied.[18] For highly viscoelastic materials, this can be complex, because the extensional viscosity of the fluid will also contribute to the force generated. The plate can be left at the interface for the slurry to relax and these forces to dissipate, but care must be taken as this can take long times over which drying can occur, and some slurries have yield stress which means the forces may not fully dissipate.

Contact angle is easier to determine, from imaging of a droplet of slurry on current collector. Measurements on different surfaces with known surface energy can also be used to extract the surface tension of the liquid. However, there can be complications in dispensing the drop, because the slurries are viscous, and contain large particles. A very small drop (under 10 microlitres) is typically used to avoid gravitational slumping, so care must be taken to ensure that this small amount can be dispensed reproducibility and is representative of the bulk
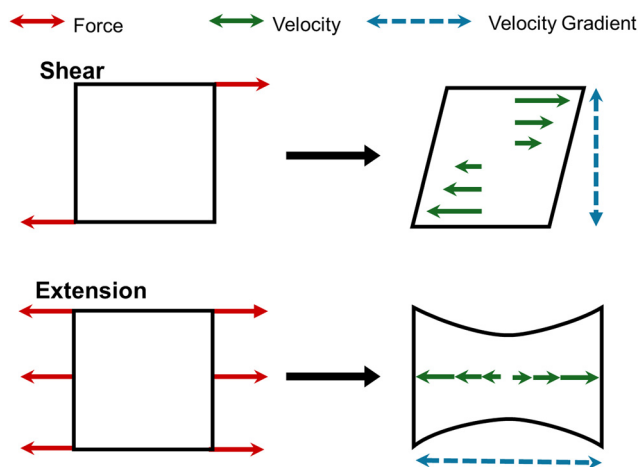
Fig. 3 Illustration of shear and extensional flows.

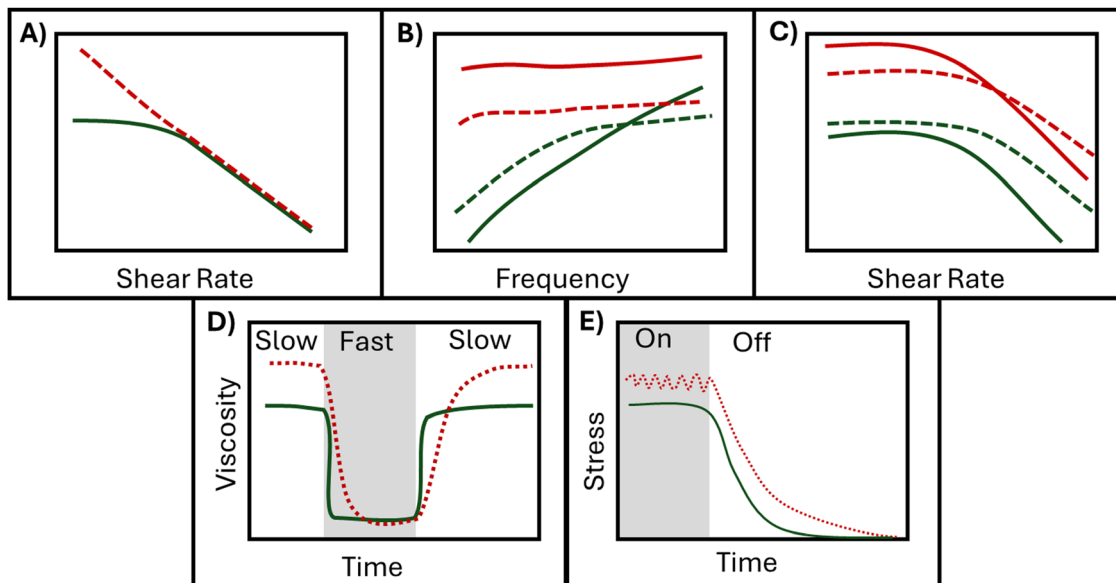Legend: Force, Velocity, Velocity Gradient
Shear
Extension

Fig. 4 Example shear rheology measurements that can be made to extract key parameters, using two example systems to illustrate. The red curves represent a high viscosity yield stress slurry, which likely contains a network structure which breaks up on shear. The green curves represent a well dispersed slurry where the particles do not form a network and the behaviour is similar to a well dispersed dissolved polymer binder. (A) Flow curve, which can be fitted with models. The gradient indicates steepness of shear thinning. The lack of a low shear plateau indicates yield stress behaviour. (B) Frequency sweep, where parallel lines with $G' > G''$ indicate gel like behaviour. A crossover occurs when a relaxation time is exceeded. (C) Amplitude sweep, which can be used for extraction of the yield stress. (D) 3ITT which can be used to indicate recovery after shear. (E) Relaxation after cessation of a steady shear. The presence of undulations in the initial plateau may indicate instability (this raw data can also be analysed from a flow curve), and the relaxation can be fitted to extract relaxation times that are exceeded at the shear rate used.
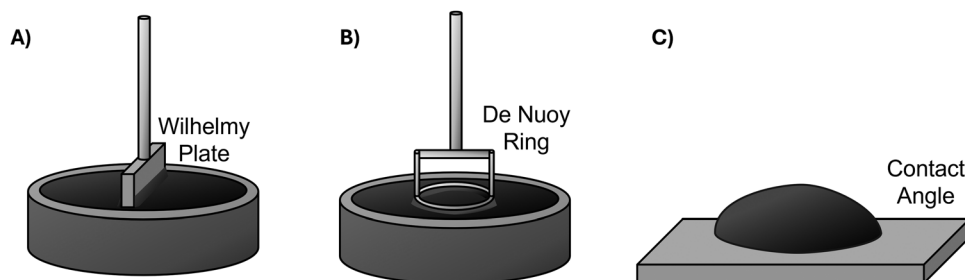

Fig. 5 Illustration of surface property measurements (A) Wilhelmy plate, (B) de Nuoy ring and (C) contact angle measurement.

(*e.g.* by using pipette tips larger than agglomerate size and giving time for relaxation during drawing and dispensing of drops). Surface tension can also be measured from imaging dispensed drops, in the drop volume approach – similar care needs to be taken here to ensure the dispensed drops are representative.

In cases where the surface properties cannot be measured, estimates can be used from other samples or literature to obtain a range, and then sensitivity to surface tension can be checked in the modelling approach.

Microstructural assessment

Slurry rheology is determined by the microstructure of the added components, so it is also useful to briefly mention the methods of microstructural assessment used for electrode slurries.

The majority of studies use scanning electron microscopy (SEM) of the dried electrode to assess the distribution of

components. However, the microstructure can change during drying, so this may not always be representative of the origins of the slurry rheology. There are advanced techniques that seek to image the slurry in a hydrated state, for example cryoSEM, which uses fast freezing and imaging under low temperature.[19,20] However there still could be a change in microstructure from the freezing process and measurement at low temperature.

The wet slurry can also be imaged using light microscopy.[21,22] Optical microscopes can image the slurry under real conditions, however the opacity of the slurry mean usually only a thin surface layer of the particles can be seen, and the resolution is limited so usually only the active material can be imaged, with the binder and conductive additive being beyond the measurement resolution.

The particle size distribution in the slurry can be useful to measure, to assess the formation of agglomerates. This can be

measured using light scattering methods, however these are again limited by opacity, and so require dilution to use, which can change the agglomeration and adsorption behaviour. A simple method that can be used on the undiluted slurry is a Hegman gauge, where the slurry is scraped through an increasingly narrow channel, so will only reach the point where the agglomerate size equals the channel gap, after which the channel will be blocked. This is also useful to predict coating behaviour as it shows which coating gaps the slurry will effectively flow through. However, it is a manual method with significant variation between users and is limited in the data that can be extracted. Automated methods for Hegman gauge are however beginning to emerge which improve reproducibility and use image analysis to produce distributions of agglomerate size rather than single point measurements.[23]

Finally, the microstructure can be inferred from bulk properties, as well as rheology and surface properties, the electrochemical behaviour of the slurry can be investigated, *e.g.* using impedance spectroscopy to probe the conductive networks within the slurry.[24] The bulk properties of the dried film can also be used (*e.g.* mechanical properties, conductivity, adhesion), but this suffers from the same problem as SEM, where the effect of drying cannot be removed.

Rheology during electrode manufacturing

Electrode slurry formulation. The slurry formulation most commonly consists of the active material, a conductive additive, a polymeric binder, and sometimes further additives for dispersion and/or electrochemical performance, which are all dispersed in a solvent. There are a huge range of active materials used in battery manufacture, some examples are lithium iron phosphate or nickel manganese cobalt oxides for lithium cathodes,[25] and graphite[26] or silicon oxides (or blends of the two) for lithium anodes. Alternative chemistries to lithium are also becoming more common, with sodium batteries beginning commercial production, which may use hard carbon as the anode and Prussian white or layered transition metal oxides as cathode.

The active material is the largest component of the formulation (other than solvent, dependant of the weight solids used), and so would be expected to have a larger impact on bulk properties. However, this is not always the case, rheological properties for example have been shown to be mostly determined by the carbon-binder networks in the slurry.[27] Nevertheless, there is a huge potential for variation between active materials and the most common drivers of changes to the slurry properties, are the particle size and shape distribution, and surface chemistry.

The particle size and shape are vitally important properties of the active. The first impact this has is on the packing of the particles. Smaller particles have more surface area to form a network spanning the slurry, which can create gel-like properties and impart a yield stress to the slurry, a stress that must be exceeded to overcome particle–particle interactions and start flow. For example, nanoscale LFP was found to have a yield stress in PVDF and NMP alone, where micron sized NMC did not.[25] Similarly, nanosized Silicon active is seen to display higher low shear rate viscosity, characteristic of yield stress behaviour, where microscale silicon displays zero shear viscosity behaviour.[28] Surface area can also provide area for other components to absorb to *e.g.* binder, conductive additive, which can remove them from solution and change the rheology.[29] Shape is also important, in comparisons of spherical natural graphite *versus* flaked synthetic graphite, the flakes had a higher surface area for network formation at low weight solids, and gave more viscoelastic behaviour, however at high weight solids, the flakes were able to pack together more effectively than the spheres, leading to smaller effective particle volume and lower viscoelasticity.[30]

Many active materials are coated with carbon to provide conductivity but also to improve processability and limit the difference between materials that may be dropped into the standard manufacturing process. However, the chemistry of the particles is still key. An important example here is High Nickel cathode materials, which catalyse defluorination and crosslinking of PVDF binder, leading to gelation – evolution of the rheology from a free flowing slurry to a highly elastic gel.[31] The timescale of this process depends on the protective coating applied to the active, the mixing process which can further protect the material, and the moisture content of the atmosphere the slurry is processed in.

The polymeric binder is added to thicken the slurry to suspend the components and prevent settling. It also provides mechanical properties in the dried electrode, such as flexibility and adhesion of the coating to the current collector. Some of the most common battery binders are PVDF, which is insoluble in many solvents, so must be processed in NMP, and CMC and SBR, usually used as a pair in water as solvent, where the CMC provides thickening of the slurry and the SBR is suspended in water and provides flexibility and adhesion of the dried electrode. However, the quantity of possible binders is immense, and the literature has utilised a wide range of synthetic and natural polymers for this purpose.

The key properties of the binder that influence the slurry rheology are the molecular weight, the presence of branching and the polymer chemistry. For linear polymers, the viscosity increases with molecular weight (in fact viscosity is commonly used to determine polymer molecular weight).[32,33] The presence of branch points hinders the relaxation of entanglements between polymers, causing longer relaxation times and higher viscosities. Branched polymers can therefore thicken solutions in very small amounts.

The chemistry can be vital, as discussed previously PVDF forms crosslinks in the presence of certain active materials, which makes the rheology change over time. Increasing degree of substitution of CMC shows a decrease in tendency to adsorb onto graphite active particles and thus increases free polymer in solution and viscosity.[34] Changing the polymer from PVDF to polyvinyl pyrrolidone increases the tendency to adsorb to and disperse carbon black particles in the slurry, breaking up conductive networks.[35] In water based anode slurries, both CMC and SBR adsorb to Graphite surfaces, but CMC is preferential to SBR and can displace SBR.[19]

The conductive additive can also contribute, which is often carbon black, although nanotubes, graphene or a small particle size graphite are sometimes used. This component, added in small amounts for conductivity, may seem an unlikely contributor to the bulk rheology, however, due to its small particle size, it has high surface area, and only small amounts are needed to form a conductive network through the slurry, which can also contribute to the mechanical properties. In NMP solvent, carbon black is known to disperse without the addition of surfactant[36] as the surface charges match well with the intermediate polarity of the solvent, so the particles form a network spontaneously in solvent alone.[25] This network has been detected by slurry impedance measurements and seen to break up with high shear.[24] These networks have also been imaged by transmission electron microscopy.[26]

In NMP, this conductive additive network contributes a large portion of the rheological behaviour, and the other components serve to remove or free up carbon black to form a network in solution.[4,37] Bauer and Nötzel found that dry blending the active with Carbon black made the carbon adhere to the active material rather than being free in solution, which removed the gel-like behaviour provided by the CB network.[25] Increases in yield stress have been observed when increasing CB and PVDF content but not when increasing active content for LFP slurries.[38] The size and shape of these additives is also important, network formation (and yield stress) is seen to be promoted by small sizes and high aspect ratio shapes (*e.g.* nanotubes).[39]

The ratio of components and solvent is of course vital to maintaining the effects discussed for each component. The weight or volume fraction of a slurry is an important and particle–particle interactions increase with weight solids, leading to increases in viscosity and yield stress.[40] However, different components can contribute at different solids loadings. For high nickel cathode slurries is shown to increase significantly with weight fraction. At the highest weight fractions agglomerate size is seen to increase which suggests this is due to the formation of a particle–particle network, however in an intermediate region agglomerate size is constant, so the yield stress likely originates from the carbon black network in the slurry.[41]

The solvent provides the background viscosity (usually Newtonian) and the capability to dissolve the binder. However secondary solvents such as 1-octanol in water have been utilised to create capillary bridges between active particles, which can induce network formation and create paste-like yield stress behaviour.[11,42–44]

The balance between component contributions is shown in Fig. 6, where example structures are shown, with all components isolated, or network formation from active, conductive additive, or binder (multi-component networks can also form). Hence, any formulation changes which shift the balance of adsorbed and free components can shift the slurry between these structures and change the rheology.

Mixing

The mixing process determines the microstructure of the slurry, with the aim being a uniform dispersion of components. Intensive mixing can break up agglomerates of active and conductive additive, however, it can also promote adsorption of binder and additive to the particle surfaces. This can be used to protect the particles or improve their conductivity or stability in solution, but overmixing can cause excessive removal of binder and conductive additive from solution, leading to loss of the conductive network and poor mechanical properties in the dry electrode.[45,46]

For binder, insufficient dispersion can cause high viscosities and elastic behaviour *e.g.* clumping of CMC in water, which is removed after further shear,[47] which carry through into poor dispersion in the dry electrode to give inconsistent mechanical properties.

The order of mixing is also vital, for example, in NMC cathode slurries, mixing the carbon black into the NMP solvent first promotes formation of a carbon black network which the active can be added into, but premixing active and carbon black promotes absorption to the active surfaces, reducing the amount of free carbon black and thus preventing network formation.[48,49] Slurry stability and age is another important consideration, settling and agglomeration is seen to occur when the slurry is aged, particularly of the carbon black, leading to loss of the conductive network and yield stress behaviour. Agitation during aging, while helping to keep
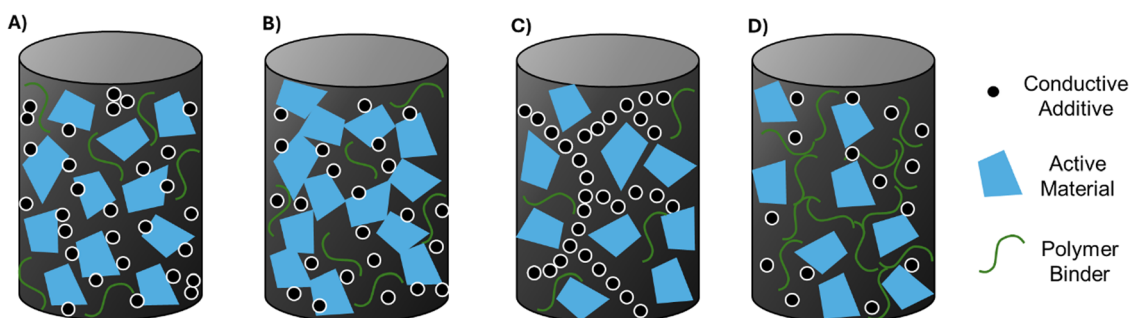

Fig. 6 Illustration of possible structures in an electrode slurry, with 3 possible routes to a yield stress network (A) conductive additive is adsorbed onto active material particles, which are well dispersed – the rheology is similar to solvent *i.e.* shear thinning with no yield stress. (B) Active material forms a network (*e.g.* for small actives like LFP) (C) conductive additive forms a network (D) binder overlaps and forms a network, 2–4 would all show yield stress behaviour after which shear thinning, the magnitude of which is dependent on the components.

Legend:
- • Conductive Additive
- ▨ Active Material
- ∿ Polymer Binder

dispersion of the active, can actually worsen this agglomeration of the carbon black.[50]

There are various ways to assess the mixing process in-line. Torque can be monitored to study the evolution of the slurry rheology, but this is a complex combination of the slurry response and effects of the mixer geometry, so must be calibrated to the setup and material. It can however be used to detect when mixing is complete for repeats of the same mix.[51] Particle tracking methods can be used to assess the flow in the mixer, this allows extraction of physical measurements from the mixing process *e.g.* energy input, shear rates, which can be related to the formulation to predict impact on the distribution of components.[52] However, due to the variety of possible parameters and formulations, even at this initial stage of the manufacturing process, the problem is complex, and there is still work to be done on elucidating the relationship between mixing parameters and final microstructure.

Coating

The slurry rheology is key to coating. High viscosity can cause excessive pressure build-up in the pipes/coater head and limits the speed of coating. Low viscosity is also a problem, as it can cause slumping after coating, leading to thin, non-uniform electrodes. Because these processes occur at different shear rates, a desirable behaviour is a steep shear thinning, having high viscosity at low shear rates *i.e.* under gravity to prevent slumping, and a low viscosity at high shear rates *e.g.* in the coater head. A yield stress is also desirable as it prevents settling of components within the slurry if left to rest between mixing and coating (*e.g.* during degassing). Prevention of settling and slumping has an impact on the final cell, for example in silicon anodes, higher molecular weight binder was seen to improve electrochemical performance but an equal affect was achieved using an alternative solvent with higher viscosity – demonstrating the change was driven by rheology.[53]

The shear rate during coating can be calculated for comparison to the rheological results. For shear in the coating gap (*e.g.* the gap between the foil substrate and the slot die head or blade) this can be calculated as the substrate speed, v divided by the gap, h: $\dot{\gamma} = \dfrac{v}{h}$. For the shear within the slot die, which is driven by the flow rate of material, Q, this becomes $\dot{\gamma} = \dfrac{6Q}{w^2 d}$, where w is the internal gap in the slot and d the slot depth (*i.e.* the width of coating produced).

The thickness profile of the coating is driven by the slurry rheology. A common problem is high or 'heavy' edges, uneven areas near the coating edges which typically exceed the average coating thickness. A uniform coating with sharp edges is desirable, so engineering the rheology is key. High edges have been shown to be removed by incorporating a yield stress network into the slurry.[11,54,55]

Elastic behaviour in the coater can cause coating instability and non-uniformity.[56] For this reason, it is important to measure a relaxation time for the slurry and compare it to the shear rate of the process. If the Weissenberg number, which is the product of the deformation rate (*e.g.* shear rate, extension rate) and the relaxation time, is above 1, the slurry is being deformed faster than it can relax, and therefore elastic instability can occur.

The rheology can also give insights into the microstructure that may aid prevention of other defects, for example agglomeration can be detected by loss of gel-like yield stress behaviour.[57] These agglomerates can accumulate in dead zones, and block the coater gap leading to streaks in the coating.[58]

Drying and calendaring

Although the impact of the slurry on these later processes is perhaps not obvious, as the solvent is now being removed, the slurry properties are key to the microstructure obtained during drying, which will go on to impact the mechanical properties during calendaring.

The drying process is thought to proceed by a two-step mechanism, consolidation of the coating where thickness is reduced, and then one the particles have consolidated into a network structure, the remaining solvent is removed *via* capillary action through the pore network.[59] One example of how rheology can be important during drying in binder migration – during drying binder can migrate away from the current collector, leading to poor adhesion.[60] Formation of networks *via* additives (which can be detected using slurry yield stress) has been shown to impede binder migration and improve adhesion.[61] This migration also gives an uneven distribution of mechanical properties across the dry coating, which can cause cracking and delamination on calendaring.

Industry perspective

According to a market study by McKinsey, the global demand for lithium-ion batteries (LIBs) is expected to grow at approximately 25% annually by 2030.[62] Despite this increase in demand and competition, the large-scale manufacturing of lithium-ion batteries remains a complex and expensive process. A critical stage in this manufacturing process chain is the coating of electrodes. Slot-die coating is commonly used for electrode coating because it provides the extreme precision and accuracy required for high-quality coating and uniformity. Unlike other coating methods, such as blade coating where the slurry is applied to the foil and excess material is scrapped off during the coating process to achieve desired thickness, slot die coating is pre-metered. This means it delivers the exact amount of slurry needed onto the substrate or foil, resulting in no wastage. Additionally, this technique is easily integrated into scalable processes, including roll-to-roll systems.

In battery manufacturing, wet coating thickness typically ranges from less than 500 μm to as low as 10 μm. For context, human hair has a nominal thickness of 50–120 μm.[63] Slot-die coating can deposit films with thicknesses spanning from a few nanometres to several microns and can manage viscosities from a few centimetres per second to several meters per second.

Uniformity of the coating film is crucial in electrode coating as it directly impacts the overall quality and performance of the
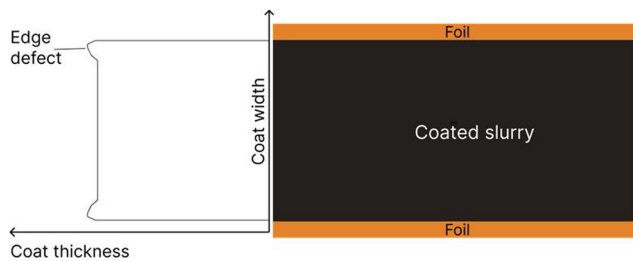
Fig. 7 Illustration of edge defect in an electrode slurry for continuous coating, superelevation at the edges of the coated slurry can be observed.

Fig. 8 Illustration of minor leaks at the mass-free zone in a coated electrode slurry for intermittent coating.

battery. Consistency in coating thickness across the foil is essential, as variations such as heavy or thick edges leading to crack initiation due to increase in local stress concentration during coil winding and calendaring are undesirable (see Fig. 7). The tolerance for transverse web thickness should not exceed a 3% variation to maintain high quality.

To avoid trial-and-error in manufacturing process, an approach that can lead to material wastage and increase in downtime, computational simulations of slot die coating are essential in the battery manufacturing process. Using a 2D or 3D model of the slot-die, the coating process can be modelled, visualised, and optimised before actual coating on the manufacturing line begins.

These simulations predict edge thicknesses and help inform slot die setup and process settings to achieve a quality coating process. Before performing simulations, understanding the rheology of the slurry to be used is vital. Different slurries behave differently, and material characterisation helps in accurately modelling and predicting the flow dynamics within the slot die and the gap between the slot die and the substrate. Standard industrial procedures for slurry characterisation involve measuring viscosity, density, surface tension, contact angle, amplitude and frequency sweep for elasticity, and thixotropic recovery.

Slurries used for coating in lithium-ion battery manufacturing are highly non-Newtonian and exhibit shear thinning properties, where the viscosity of the slurry decreases with an increase in shear rate in the narrow gap between the slot-die and the moving substrate or foil. The viscosity flow curve informs the process simulation of the rheological behaviour of the non-Newtonian slurry, which can significantly affect the steady, uniform flow of the electrode coating.

The contact angle of the slurry with the foil or substrate provides useful information about its wettability, indicating how well the slurry will spread over the foil surface. A high contact angle suggests low wettability, which correlates with defects such as edge and pinhole defects on the coating. Additionally, the surface energy of different regions within the slurry mix can also affect how the solution wets the foil surface. For slot-die coating techniques, particularly intermittent coating where periodic slurry feeding is automatically regulated by a valve to create discrete spaces between electrode patches, understanding the rheology of the slurry's viscoelastic properties is crucial.[56] This knowledge is essential to predict
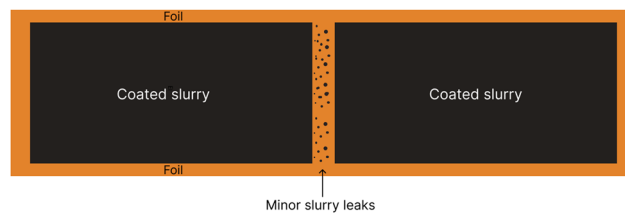
slurry's elastic behaviour particularly during the suction phase of the valve when the slurry flow is stopped abruptly to generate a mass-free zone. During the suction process, the highly elastic properties of the slurry cause it to respond more slowly during the expansion phase, resulting in a delayed return to its original state. This behaviour during the retraction phase of the coating bead can destabilise the menisci leading to pronounced trailing edges on the coated foil and minor leaks into the mass-free zone (Fig. 8).

Summary and recommendations

In summary, understanding the rheological properties and slurry microstructure is crucial to optimizing the manufacturing process of battery electrodes. The rheological properties provide valuable insights into the effectiveness of mixing and the internal structure of the slurry, including agglomeration, adsorption of components at interfaces, and the formation of particle-polymer networks. These properties play a vital role in determining the performance of the slurry in subsequent manufacturing steps such as coating and drying.

The formulation and mixing processes significantly influence the dominant rheological characteristics and the microstructure of the slurry. Minor adjustments in component ratios or processing techniques can lead to substantial changes in the slurry's properties and performance. The microstructure, characterized by the distribution and interaction of particles within the slurry, directly impacts the quality of the final product, affecting coating thickness, uniformity, and the presence of defects.

Key recommendations for advancing the study and measurement of slurry properties, microstructure, and metrology include:

• Developing comprehensive datasets that map the effects of formulation and process parameters on the manufacturing process, thereby providing a deeper understanding of the relationships between these variables and the resulting slurry properties.

• Enhancing methods for assessing microstructure, such as using optical microscopy for slurry and SEM for dried electrodes, to capture changes due to formulation and mixing procedures. This will help in correlating the microstructure with performance outcomes.

• Regularly measuring slurry agglomerate size in a reproducible manner, avoiding dilution to minimize user variation. Automated methods can be employed to improve the reliability and consistency of these measurements.

• Improving rheological measurements by including high shear rate assessments, (*e.g.* by carefully reducing parallel plate gaps or capillary rheometry), and considering oscillatory rheology and yield stress quantification. Both shear and extensional properties should be measured to provide a comprehensive understanding of the slurry behaviour.

• Routinely assessing surface properties, despite the challenges in measuring them for highly viscoelastic slurries. Surface tension is critical for the physical modelling of the process and should be integrated into the analysis.

By focusing on these areas, researchers and manufacturers can optimize the rheological properties and microstructure of electrode slurries, leading to better manufacturing outcomes and enhanced performance and reliability of the produced electrodes.

Data availability

No primary research results, software or code have been included and no new data were generated or analysed as part of this review.

Conflicts of interest

There are no conflicts of interest to declare.

Acknowledgements

References

1 Processing and Manufacturing of Electrodes for Lithium-Ion Batteries, IET Digital Library, 2023.

2 C. D. Reynolds, P. R. Slater, S. D. Hare, M. J. H. Simmons and E. Kendrick, *Mater. Des.*, 2021, **209**, 109971.

3 E. Kendrick, *Future Lithium-ion Batteries*, 2019, pp. 262–289.

4 C. D. Reynolds, S. D. Hare, P. R. Slater, M. J. H. Simmons and E. Kendrick, *Energy Technol.*, 2022, **10**, 2200545.

5 T. Schweizer, *Rheol. Acta*, 2002, **41**, 337–344.

6 O. J. Romero, L. E. Scriven and M. S. Carvalho, *J. Non-Newtonian Fluid Mech.*, 2006, **138**, 63–75.

7 O. J. Romero, W. J. Suszynski, L. E. Scriven and M. S. Carvalho, *J. Non-Newtonian Fluid Mech.*, 2004, **118**, 137–156.

8 V. Chu, M.-Z. Tsai, Y.-R. Chang, T.-J. Liu and C. Tiu, *J. Appl. Polym. Sci.*, 2010, **116**, 654–662.

9 M. Bajaj, J. Ravi Prakash and M. Pasquali, *J. Non-Newtonian Fluid Mech.*, 2008, **149**, 104–123.

10 R. Diehm, M. Müller, D. Burger, J. Kumberg, S. Spiegel, W. Bauer, P. Scharfer and W. Schabel, *Energy Technol.*, 2020, **8**, 2000259.

11 B. Bitsch, J. Dittmann, M. Schmitt, P. Scharfer, W. Schabel and N. Willenbacher, *J. Power Sources*, 2014, **265**, 81–90.

12 H. J. Walls, S. B. Caines, A. M. Sanchez and S. A. Khan, *J. Rheol.*, 2003, **47**, 847–868.

13 M.-C. Yang, L. E. Scriven and C. W. Macosko, *J. Rheol.*, 1986, **30**, 1015–1029.

14 C. D. Reynolds, J. Lam, L. Yang and E. Kendrick, *Mater. Des.*, 2022, **222**, 111104.

15 W. Jun Lee, N. Park, J. In Park, J. Nam, K. Hyun Ahn and J. Min Kim, *J. Colloid Interface Sci.*, 2024, **663**, 508–517.

16 M. Padmanabhan, C. W. Macosko and M. Padmanabhan, *Rheol. Acta*, 1997, **36**, 144–151.

17 M. Zatloukal, J. V. Vlcek, C. Tzoganakis and P. Saha, *J. Non-Newtonian Fluid Mech.*, 2002, **107**, 13–37.

18 S. Ebnesajjad and A. H. Landrock, *Adhesives Technology Handbook*, ed. S. Ebnesajjad and A. H. Landrock, William Andrew Publishing, Boston, 3rd edn, 2015, pp. 19–34.

19 S. Lim, S. Kim, K. H. Ahn and S. J. Lee, *J. Power Sources*, 2015, **299**, 221–230.

20 J. Kumberg, W. Bauer, J. Schmatz, R. Diehm, M. Tönsmann, M. Müller, K. Ly, P. Scharfer and W. Schabel, *Energy Technol.*, 2021, **9**, 2100367.

21 A. Cushing, T. Zheng, K. Higa and G. Liu, *Polymers*, 2021, **13**, 4033.

22 A. R. T. Morrison, W. Dawson, E. Kendrick, P. R. Shearing and D. Brett, *ECS Meet. Abstr.*, 2022, **MA2022-01**, 418.

23 M. K. Alazzawi, B. Beyoglu, F. F. Maniaci and R. A. Haber, *Powder Technol.*, 2021, **382**, 318–330.

24 I. Shitanda, K. Sugaya, C. Baba, N. Loew, Y. Yamagata, K. Miyamoto, S. Niinobe, K. Komatsuki, H. Watanabe and M. Itagaki, *ACS Appl. Electron. Mater.*, 2023, **5**, 4394–4400.

25 W. Bauer and D. Nötzel, *Ceram. Int.*, 2014, **40** 4591–4598.

26 J. P. Sullivan and A. Bose, *Electrochem. Commun.*, 2022, **141**, 107353.

27 J. Entwistle, R. Ge, K. Pardikar, R. Smith and D. Cumming, *Renewable Sustainable Energy Rev.*, 2022, **166**, 112624.

28 R. Andersson, G. Hernández, K. Edström and J. Mindemark, *Energy Technol.*, 2020, **8**, 2000056.

29 M. Ishii and H. Nakamura, *JCIS Open*, 2022, **6**, 100048.

30 Y. Kim, E. H. Jeong, B. S. Kim and J. D. Park, *Korea-Aust. Rheol. J.*, 2024, **36**, 25–32.

31 S. Roberts, L. Chen, B. Kishore, C. E. J. Dancer, M. J. H. Simmons and E. Kendrick, *J. Colloid Interface Sci.*, 2022, **627**, 427–437.

32 R. H. Colby, L. J. Fetters and W. W. Graessley, *Macromolecules*, 1987, **20**, 2226–2237.

33 M. Rao, *Polymer*, 1993, **34**, 592–596.

34 R. Gordon, R. Orias and N. Willenbacher, *J. Mater. Sci.*, 2020, **55**, 15867–15881.

35 S. H. Sung, S. Kim, J. H. Park, J. D. Park and K. H. Ahn, *Materials*, 2020, **13**, 4544.

36 A. Basch, R. Horn and J. O. Besenhard, *Colloids Surf., A*, 2005, **253**, 155–161.

37 F. Ma, Y. Fu, V. Battaglia and R. Prasher, *J. Power Sources*, 2019, **438**, 226994.

38 B. Zhao, D. Yin, Y. Gao and J. Ren, *J. Electron. Mater.*, 2022, **51**, 3885–3895.

39 P. Su, H. Zhang, L. Yang, C. Xing, S. Pan, W. Lu and S. Zhang, *Chem. Eng. J.*, 2022, **433**, 133203.

40 B. Zhao, D. Yin, Y. Gao and J. Ren, *Ceram. Int.*, 2022, **48**, 19073–19080.

41 L. Ouyang, Z. Wu, J. Wang, X. Qi, Q. Li, J. Wang and S. Lu, *RSC Adv.*, 2020, **10**, 19360–19370.

42 D. Gastol, M. Capener, C. Reynolds, C. Constable and E. Kendrick, *Mater. Des.*, 2021, **205**, 109720.

43 J. Park, N. Willenbacher and K. H. Ahn, *Colloids Surf., A*, 2019, **579**, 123692.

44 M. Schneider, E. Koos and N. Willenbacher, *Sci. Rep.*, 2016, **6**, 31367.

45 Y. Komoda, K. Ishibashi, K. Kuratani, R. Hidema, H. Suzuki and H. Kobayashi, *JCIS Open*, 2022, **5**, 100038.

46 D. Zapata Dominguez, J. Xu, Y. Boudjema, S. Ben Hadj Ali, F. M. Zanotto and A. A. Franco, *J. Power Sources Adv.*, 2024, **26**, 100141.

47 S. Makino, Y. Akimoto, M. Ishii and H. Nakamura, *Rheol. Acta*, 2024, **63**, 319–331.

48 M. Wang, D. Dang, A. Meyer, R. Arsenault and Y.-T. Cheng, *J. Electrochem. Soc.*, 2020, **167**, 100518.

49 M. Takemo, S. Katakura, K. Miyazaki, T. Abe and T. Fukutsuka, *Electrochemistry*, 2021, **89**, 585–589.

50 Y. I. Kwon, J. D. Kim and Y. S. Song, *J. Electron. Mater.*, 2015, **44**, 475–481.

51 D. Grießl, A. Adam, K. Huber and A. Kwade, *J. Electrochem. Soc.*, 2022, **169**, 020531.

52 S. D. Hare, D. Werner, C. R. K. Windows-Yule, T. Z. K. Wheldon, E. Kendrick and M. J. H. Simmons, *Chem. Eng. Res. Des.*, 2023, **197**, 509–518.

53 H. Jiang, C. Wei, S. Yasmin and M. N. Obrovac, *J. Electrochem. Soc.*, 2023, **170**, 120522.

54 P. Galek, J. Różański and K. Fic, *Chem. Eng. J.*, 2023, **463**, 1–10.

55 S. Spiegel, T. Heckmann, A. Altvater, R. Diehm, P. Scharfer and W. Schabel, *J. Coat. Technol. Res.*, 2022, **19**, 121–130.

56 M. Schmitt, Slot die coating of lithium-ion battery electrodes, **https://publikationen.bibliothek.kit.edu/1000051733**, (accessed 7 June 2024).

57 J. H. Park, S. H. Sung, S. Kim and K. H. Ahn, *Ind. Eng. Chem. Res.*, 2022, **61**, 2100–2109.

58 C. D. Reynolds and E. Kendrick, *Processing and Manufacturing of Electrodes for Lithium-Ion Batteries*, IET Digital Library, 2023, pp. 339–367.

59 A Review of Lithium-Ion Battery Electrode Drying: Mechanisms and Metrology - Zhang - 2022 - Advanced Energy Materials – Wiley Online Library, **https://onlinelibrary.wiley.com/doi/full/10.1002/aenm.202102233**, (accessed 7 June 2024).

60 F. Font, B. Protas, G. Richardson and J. M. Foster, *J. Power Sources*, 2018, **393**, 177–185.

61 D. Burger, J. Klemens, N. Keim, M. Müller, W. Bauer, J. Schmatz, J. Kumberg, P. Scharfer and W. Schabel, *Energy Technol.*, 2024, 2400057.

62 Lithium-ion battery demand forecast for 2030 | McKinsey, **https://www.mckinsey.com/industries/automotive-and-assembly/our-insights/battery-2030-resilient-sustainable-and-circular**, (accessed 12 June 2024).

63 J. H. Park, Y. H. Ho and K. Manonukul, *Arch. Aesthetic Plast. Surg.*, 2023, **29**, 97–101.